Energy Proceedings
Vol 39, 2024
ISSN 2004-2965

Improving the performance of a pumped hydro storage plant through integration with floating photovoltaic

Matteo Catania[1*], Abdullah Bamoshmoosh[1], Vincenzo Dipierro[1], Marco Ficili[1], Andrea Fusco[1], Domenico Gioffré[1], Federico Parolin[1], Lorenzo Pilotti[1], Ferdinando Vincenti[1], Andrea Zelaschi[1]

1 Department of Energy, Politecnico di Milano, Via Lambruschini 4A, 20156 Milan, Italy

(*corresponding author: matteo.catania@polimi.it)

ABSTRACT

This study investigates the techno-economic optimization of Pumped Hydro Storage (PHS) with integrated Floating Photovoltaic (FPV) systems, emphasizing two configurations. FPV modules, installed over water basins, exploit unused space, reducing water evaporation and enhancing photovoltaic efficiency via natural water-cooling. The Capriati PHS plant in Italy serves as the study case due to favorable irradiation conditions. The FPV model considers water cooling's positive impact on PV cell efficiency and basin surface evaporation reduction. Historical meteorological data inform FPV production profiles, guiding an hour-based yearly optimization. Results reveal a substantial PHS utilization increase. In the first configuration, connecting FPV to the pump boosts Net Present Value and Equivalent Operating Hours (EOH) by around 60% and 40%, respectively. In the second configuration, grid interaction and electricity export lead to a 90% NPV increase and a 20% EOH increase. PHS-FPV integration enhances both PV and PHS productivity, offering a solution to challenges posed by seasonal PV production fluctuations.

Keywords: PV, PHS, FPV, floating photovoltaic, energy storage, optimization.

NONMENCLATURE

Abbreviations	
ASM	Ancillary Services Market
ASR	Available Surface Ratio
CAPEX	Capital Expenditure
DAM	Day-Ahead Market
EOH	Equivalent Operating Hours
FPV	Floating Photovoltaic
GHI	Global Horizontal Irradiation
KPI	Key Performance Indicator
MILP	Mixed-Integer Linear Programming
NOCT	Nominal Cell Operating Temperature
NPV	Net Present Value
O&M	Operations and Maintenance
OPEX	Operational Expenditure
PHS	Pumped Hydro Storage
PV	Photovoltaic
STC	Standard Test Conditions
TAC	Total Annual Cost
Symbols	
E	Evaporation rate
R_s	Global horizontal radiation
T	Ambient temperature
w	Wind speed

1. INTRODUCTION

The imperative of the global energy transition, driven by the need to combat climate change, underscores the urgency of deploying cleaner and more sustainable energy sources. In this context, there is a growing demand for the expansion of PV solar and wind power installations to reduce carbon emissions and meet rising energy needs. However, traditional land-based installations face challenges related to land use conflicts and complex permitting processes. To address these issues, FPV systems offer a promising solution. By utilizing water bodies such as reservoirs, lakes, and ponds, these systems minimize land-use and streamline permitting issues, making them an attractive option for renewable energy expansion. Moreover, the integration of FPV panels with PHS plants presents a unique opportunity for synergy. This hybrid approach allows for better energy management through the combination of solar power and hydroelectric storage, reducing water

This is a paper for 15th International Conference on Applied Energy (ICAE2023), Dec. 3-7, 2023, Doha, Qatar.

evaporation from the reservoir due to panel shading, and enhancing panel efficiency through cooling effects. This integration holds the potential to revolutionize the renewable energy landscape by providing a sustainable and efficient hybrid solution that benefits both the environment and energy production.

In recent years, the integration of floating solar panels with hydroelectric power plants has gained substantial attention in the literature. Several early studies [1–3] explored the technical feasibility of FPV technology. These works laid the foundation for understanding the practical aspects of deploying solar panels on water surfaces. On the economic front, Baptista et al. [4] conducted a techno-economic analysis, particularly in Southern European contexts, assessing the viability of FPV installations. Cazzaniga [5] considered economic factors, examining the integration of compressed air energy storage with FPV plants. Researchers have also investigated the integration of floating PV with hydroelectric power plants. Pianco et al. [6] conducted a case study focusing on the synergies and benefits of this integration, while Liu et al. [7] highlighted the advantages of combining FPV and PHS systems.

In conclusion, recent literature reflects a growing interest in floating PV, especially in conjunction with hydroelectric power. While significant strides have been made in understanding technical and economic feasibility, further research opportunities exist to optimize these integrated energy generation systems.

The aim of the work is to produce a model that can consider all the variables related to the hybridization of PHS plants and FPV to understand the technical and economic feasibility of the system. The present work aims to unveil the technical and economic feasibility of this kind of hybridization by using a Mixed Integer Linear Programming (MILP) optimization model.

Section 1 of the paper is devoted to the introduction. Section 2 deals with the model description and the report the data used to set up the case study. Section 3 explores the results of the study and Section 4 closes the paper with conclusions and future works.

2. METHODS AND DATA

2.1. Plant description

The general scheme of the model developed in this work is depicted in Figure 1, which shows the presence of both PHS and FPV systems. The PHS system comprises the turbine, the pump, and the upstream and downstream basins. Pump and turbine are connected to the electrical grid to buy and sell electricity, respectively. Moreover, floating PV panels can be installed and connected to both the electrical grid (to sell the produced electricity) and to the pump (to self-consume the renewable production to run the pump instead of buying electricity from the grid).

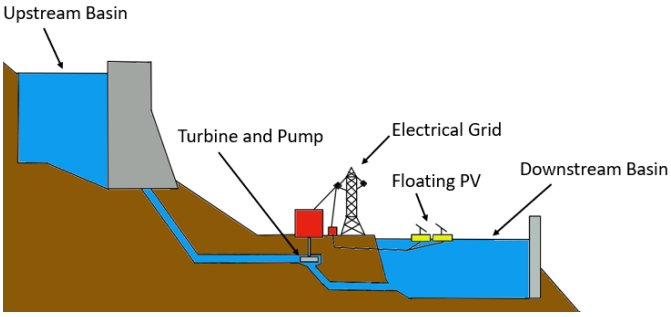

Fig. 1. PHS-FPV plant layout.

2.2. PHS model

The PHS system is modelled considering three main components: water storage, turbine, and pump. From the modelling perspective, the water storage is seen as a single water tank representing the entire water volume that could be moved between the upstream and downstream basin: if a given water content is present in the upper basin at a certain time instant, it can be sent to the turbine to generate electrical power until the storage is empty. Once the water storage is completely empty, the turbine cannot generate power (because there is no further water volume available to run the turbine), and the only possibility is to recharge it by running the pump. As for the turbine, the electrical power output is dependent on the inlet water volumetric flow rate by means of static head, water density, gravity acceleration, hydraulic efficiency (assumed constant, i.e., independent on the part-load ratio of the turbine), mechanical efficiency of shaft and electrical efficiency of the alternator. A similar relationship is defined for the pump but considering electrical power input (generated by the electrical motor) and outlet water volumetric flow rate to recharge the water storage. At a given time instant, the turbomachinery group (pump + turbine) can be run either in turbine mode or in pumping mode, which means that pump and turbine of the same group cannot work simultaneously. Finally, the possibility of defining more than one pump + turbine group is implemented in the optimization model.

The ratio between turbine electrical power output and pump electrical power input represents the roundtrip efficiency of the entire PHS system. The resulting PHS roundtrip efficiency is about 72%, in the range of values reported by the literature [8]. Table 1 shows the other technical parameters for the PHS modelling, together with the variable O&M costs. No

installation cost is considered for the PHS since the plant is assumed to be already present.

The optimization model also accounts for water evaporation from the basins. The evaporation model, specific for free water basins, is described by an empirical correlation derived by Scavo et al. [9], reported in Equation (1).

$$E = 1.802 + 0.047R_s - 0.133T - 0.146w + 0.028R_sT + 0.012R_sw + 0.013Tw + 0.003R_s^2 + 0.06T^2 + 0.001w^2 \quad (1)$$

The evaporation rate (E) is a function of the global horizontal radiation (R_s), the ambient temperature (T), and the wind speed (w). One of the positive effects of placing PV panels on a water basin is the reduction in the water evaporation rate, allowing the save of significant quantities of water in the basin. Similarly to Ref. [9], a negligible evaporation rate is assumed for the portion of basin surface covered by non-tilted PV panels.

2.3. FPV model

A Tiger Pro 60 HC multi-crystalline silicon module is chosen for PV panels. This technology features an electric efficiency of 20.39% in Standard Test Conditions (STC) [10]. A flat panel configuration is selected (0° tilt) and oriented towards the South, with an optimized azimuth angle of -6°C. This flat orientation allows to maximize the active surface covered by the PV panel with respect to the total surface required, allowing to consider an almost unitary active over gross area ratio. The expected specific PV production profile for each hour of the meteorological year (2019) is computed with the Nominal Operating Cell Temperature (NOCT) method. Weather and irradiance data is retrieved from PVGIS [11]. In addition, the operating cell temperature is adjusted to consider the effect of water cooling, using the correlation derived by Kamuyu et al. [12].

Table 1 reports the techno-economic parameters of the FPV and PHS technologies assumed in this study.

Table 1. Techno-economic parameters of PHS and FPV technologies.

Parameter	Value	Ref.
Pumped Hydro Storage		
Pump hydraulic eff. [%]	85	Assumed
Turbine hydraulic eff. [%]	90	Assumed
Roundtrip efficiency [%]	72	Computed
Variable O&M [€/MWh]	0.22	[13]
Floating Photovoltaic		
PV model	Tiger Pro 60HC	[10]
Nominal Power [kW]	0.44	
STC efficiency [%]	20.39	
Tilt/Azimuth angle [°]	0 /-6	
CAPEX (2 MW) [€/kW$_{peak}$]	1344	
CAPEX (5 MW) [€/kW$_{peak}$]	1168	
CAPEX (10 MW) [€/kW$_{peak}$]	1032	[14]
CAPEX (50 MW) [€/kW$_{peak}$]	840	
Fixed OPEX [€/kW/y]	12.4	

2.4. Optimization model

The optimization problem is tackled via a MILP model that allows to optimize the design and the operation of the plant. The problem formulation can be concisely stated as follows. Given:

- The historical hourly-resolved meteorological data (irradiance, ambient temperature, and wind speed) of the plant location.
- The historical hourly-resolved electricity sale prices and purchase costs.
- The performance and O&M cost data of the PHS units (turbines and pumps) and the floating PV system techno-economic data.
- The electric grid import/export limitations, the expected lifetime, and the system's relevant financial and economic parameters.

The model seeks to determine:

- The optimal size of the floating PV to be installed and coupled with the existing PHS.
- The commitment status (i.e. on/off, start-up, shut-down) and the optimal scheduling (i.e. generation/load, energy exchanges) of the units (FPV, pumps and turbines) at each timestep.
- The electricity to be imported/exported at each timestep.
- The water level variation in the upper basin over the entire year.

The objective is to maximize the NPV while ensuring the energy and water balances, along with other relevant constraints within the system.

2.5. Case study: Capriati plant

The developed optimization model is applied to investigate the integration of FPV with the PHS plant of Capriati, in Italy. Capriati is situated in Campania, a region of southern Italy and it has been selected among the other Italian PHS plants due to the excellent solar irradiance in the area (yearly GHI of 1565 kWh/m^2) and a relatively high average ambient temperature throughout the year (13.6 °C) that prevents the basin from possible water freezing issues. The hydroelectric plant features have been collected starting from an existing dataset used in [15] and are listed in Table 2.

Table 2. Capriati hydroelectric power plant features.

Parameter	Value
Discharge capacity [MW]	120
Pumping capacity [MW]	113
Number of groups	2
Volume upstream basin [Mm3]	8.55
Volume downstream basin [Mm3]	4.80
Head [m]	654
Downstream basin surface [km2]	0.11
Market Bidding Zone	Centre-South

Capriati has two separate groups connecting the two basins, each with similar capacities for both water pumping and discharge. For the FPV installation only the surface of the downstream basin is considered available, because it is located in proximity to the PHS pumps and to the grid connection point (see Figure 1). This choice allows to contain the need of infrastructure addition.

To remunerate the plant electricity production, the electricity prices relative to the Centre-South zone of the Italian Day Ahead Market (DAM) are considered to optimize the plant scheduling. The historical values related to the same year of reference of weather data (2019) are taken [16] and a price scaling factor of 2 is applied in order to replicate the price volatility of the current Italian electricity market (in 2022 an average value of 303 €/MWh was registered in the DAM). Such electricity price may also be representative of a future electricity market, characterized by a large presence of renewables, where the capability of PHS plant to provide dispatchable power in absence of renewable generation is expected to be highly remunerated not only in the DAM and but also in the Ancillary Services Market (ASM). Finally, the electricity purchase price is assumed to be 50% higher than the hourly zonal DAM price in order to account for grid transmission and infrastructure costs.

2.6. Analyzed configurations

The assessment considers three alternative configurations to evaluate the impact of FPV integration on the PHS plant performance. These are:

1. Case 1: the conventional PHS plant without FPV integration, which serves as reference case for the comparison.
2. Case 2: a pump-connected configuration of the FPV system, in which FPV electricity can only be used to power the PHS pump.
3. Case 3: a grid and pump-connected configuration of the FPV system, in which the connection with the grid is enabled and FPV electricity, in addition to powering the PHS pumps, can be sold to the grid.

3. RESULTS AND DISCUSSION

The optimization model described in Section 2 is applied to investigate the possibility to integrate FPV systems in the Capriati PHS plant in Southern Italy. In Section 3.1, the performance of the integrated system is compared with the conventional operation of the PHS plant considering both the pump- and the grid- and pump-connected configurations. Subsequently, to extend the validity of the obtained results, a sensitivity analysis on the available surface for FPV installation is performed in Section 3.2.

3.1. Cost-optimal design and operation of hybrid PHS-FPV system

Optimization results are obtained for the three configurations presented in Section 2.3, considering a year-long operation with hourly resolution. The available surface for FPV installation is assumed to be equal to 80% of the downstream basin surface. This results in an available surface ratio (ASR) equal to 0.8, corresponding to a maximum FPV capacity of 17.9 MW.

Table 3 provides an overview of the main Key Performance Indicators (KPI) of the plant. Results show that FPV installation positively impacts the plant economics, as the available surface is saturated in both the pump-connected and the grid- and pump-connected configurations (cases 2 and 3). The integration of the PHS plant with FPV yields a net cash flow increase of 56% and 89% in case 2 and case 3, respectively. Correspondingly, the payback time of FPV installation is equal to 8 years for case 2 and is reduced to 7 years for case 3.

In the pump-connected configuration (case 2), FPV electricity is used to drive the PHS pumps in the central hours of the day, as visible in Figure 2 showing the plant operation during three consecutive days of the year during which the storage level of PHS is progressively increased. As a result, the upper basin is filled significantly more frequently than in the reference case and the plant EOH increases by nearly 40%. In the grid- and pump-connected configuration (case 3), the FPV generation is evenly distributed between pumping and sale, with the latter being favored in the hours with peak electricity prices. Also in this case, system integration leads to an improved operation of the PHS plant, whose EOH increase by more than 20% compared case 1.

Avoided evaporation constitutes an additional benefit of FPV installation. By covering the entire available surface, the fraction of evaporated water in the downstream basin decreases from 9.3% to 1.9%.

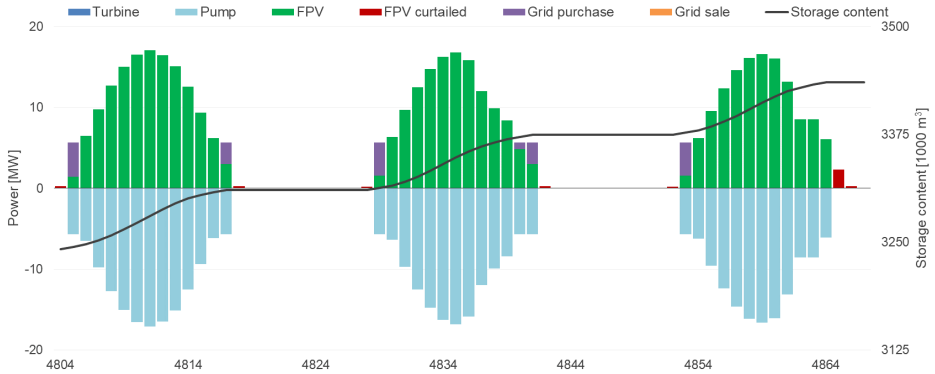

Fig. 2. Example of three consecutive days of plant operation for the pump-connected configuration (case 2).

As a result, approximately 0.4 million cubic meters per year are saved with respect to case 1, corresponding to an additional electricity generation of nearly 1 GWh/y.

Table 3. Main KPIs of the three investigated configurations.

Parameter	Case 1	Case 2	Case 3
Available surface ratio (ASR) [-]	-	0.8	0.8
FPV capacity [MW]	-	17.9	17.9
Water evaporation fraction [-]	9.3%	1.9%	1.9%
FPV generation [GWh/y]	-	28.6	28.6
FPV to pumps [GWh/y]	-	27.4	14.3
FPV to grid [GWh/y]	-	-	14.3
FPV curtailment [GWh/y]	-	1.2	0
Grid to pump [GWh/y]	47.1	37.5	42.5
PHS discharged energy [GWh/y]	33.8	46.5	40.7
PHS equivalent cycles [cycle/y]	4.5	6.2	5.5
PHS equivalent hours [h/y]	281	388	339
Net cash flow [M€/y]	1.4	2.2	2.6
Net cash flow variation [-]	-	56%	89%
NPV [M€]	14.8	23.1	28.0
FPV payback time [y]	-	8	7

3.2. Sensitivity analysis on the available surface for FPV installation

The results presented in Section 3.1 show that the system fully exploits the possibility to install FPV, saturating the available surface. This section investigates the impact of the available surface on the cost-optimal system configuration and performances. To serve this purpose, the ASR parameter is varied from 0.2 to 2.0. Values above one may correspond to either exploiting the surface of both the downstream and upstream basin or to considering a different plant with a larger basin.

Results of the analysis are summarized in Figure 3a for the pump-connected configuration and in Figure 3b for the grid- and pump-connected configuration. The system behavior is analyzed considering four parameters:

- FPV-pump size ratio, defined as the ratio between the installed FPV capacity and the nominal capacity of the PHS pump.
- FPV-pumping ratio, defined as the ratio between the amount of FPV electricity exploited for pumping and the total pumping consumptions.
- FPV-grid ratio, defined as the ratio between the amount of FPV electricity sold to the grid and the total FPV electricity generation, net of curtailment.
- the EOH of the PHS plant.

3.2.1. Pump-connected configuration

As Figure 3a shows, FPV is not installed for ASR lower than or equal than 0.2, since the generated electricity would be lower than the pump minimum technical load for most of the year. For larger values of ASR (ASR ≥ 0.4), the available surface is always saturated, as a larger FPV size yields higher PHS equivalent hours and revenues. The FPV-pumping ratio increases correspondingly, reaching nearly 75% for an ASR equal to two.

An extreme case with unbounded FPV size has also been analyzed in order to assess whether the installed FPV reaches a maximum value. Results feature an installed FPV size that matches the pump nominal capacity, showing that the system tends to maximize the FPV utilization to minimize the purchase of grid electricity. The resulting ASR is approximately 6, corresponding to the full occupation of both the upstream and downstream basins in the analyzed plant.

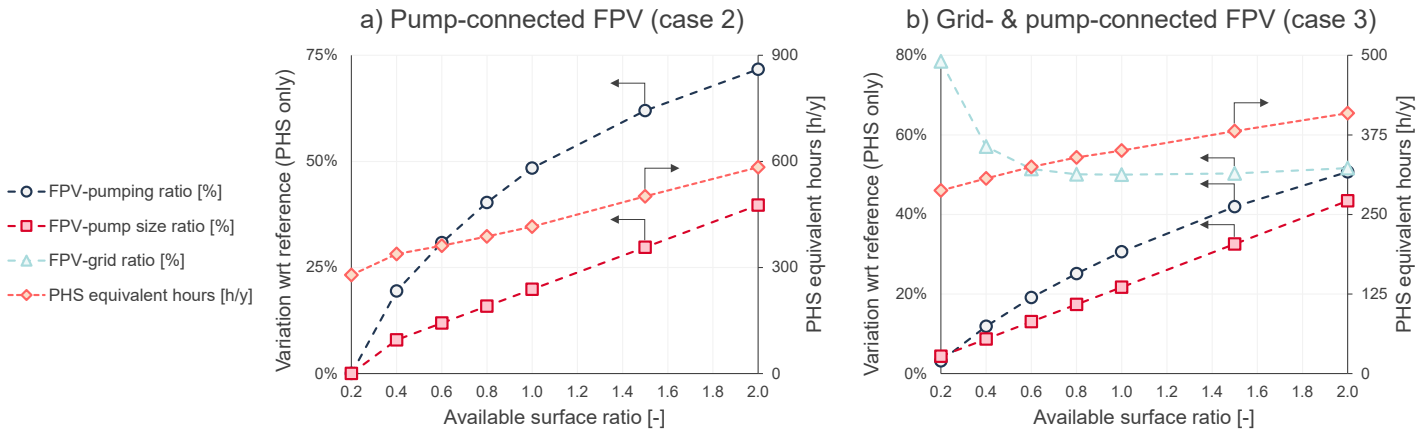

Fig. 3. Results of the sensitivity analysis on the available surface for FPV installation.

3.2.2. Grid- and pump-connected configuration

The available surface for FPV installation is always saturated if the possibility to sell FPV electricity is enabled. As Figure 3b shows, the system favors the sale of FPV electricity if the available surface is low (ASR ≤ 0.4), since the FPV-grid ratio exceeds 0.5. Conversely, the pumping operation is marginally preferred if the available surface is sufficiently high, as the FPV-grid ratio stabilizes just below 0.5 for ASR > 0.4.

Although the observed behavior strongly depends on electricity price profiles, results of this analysis show that the cost-optimal plant management involves the integrated operation of the PHS and FPV systems. Notably, using FPV electricity for pumping proves advantageous even for large FPV installed capacities.

4. CONCLUSIONS AND FUTURE WORK

This paper investigates the possibility of integrating a FPV power plant with an existing PHS plant, with the aim of comparing the possible techno-economic benefits coming from the hybridization of the two systems with respect to the stand-alone PHS. From the mathematical point of view, an optimization problem has been developed, formulated as a MILP model, in which the FPV panels are directly connected both to the electrical grid and to the pumps, to either sell electricity or power the pumps.

The developed model has been applied to an already existing PHS system located in Capriati (Italy), featured by above-average irradiation conditions and no water freezing through the year. Different configurations have been analyzed, differing for the level of PHS-FPV integration. For all the cases the maximum free surface that can be covered by the PV panels is set equal to 80% of the downstream basin surface (ASR = 0.8). According to the results, the integration of FPV with PHS is always techno-economically viable, with the saturation of the basin available surface in both case 2 and case 3. In particular, the availability of the electricity produced from PV at low cost enhances the PHS operation, ensuring a significant increase in its EOH (up to 40% in case 2). This resulted in a higher NPV in both cases, +56% and +89% in case 2 and case 3, respectively, with respect to case 1. Additionally, avoided evaporation, achieved with the presence of PV panels on the basin free surface, helps to save 0.4 million cubic meters of water per year, corresponding to almost 10% of the water present in the upper basin.

As last step, a sensitivity analysis on the available surface for FPV installation has been conducted (varying the ASR parameter), showing that the available surface for FPV panels is always saturated to increase the PHS utilization and revenues, except for case 2 with unbounded FPV size. In this case, indeed, since no PV electricity can be sold, the FPV installed size matches the pump nominal capacity, to maximize the PHS utilization while minimizing the cost of electricity purchase.

Based on what has been done so far, and given the techno-economic benefits coming from the integration of PHS system and FPV panels, future works will address: (i) the application of the proposed method to larger PHS plants, also assessing the effect of seasonal variations on the storage level, (ii) the possibility of recycling end-of-life (i.e., low cost and low efficiency) PV panels in FPV applications and (iii) the comparison of integrated PHS-FPV system with stand-alone land-based PV power plants, to evaluate possible performance improvements in term of annual electricity generation and production curtailment.

DECLARATION OF INTEREST STATEMENT

The authors declare that they have no known competing financial interests or personal relationships that could have appeared to influence the work reported in this

paper. All authors read and approved the final manuscript.

REFERENCES

[1] J. Song, Y. Choi, Analysis of the potential for use of floating photovoltaic systems on mine pit lakes: Case study at the Ssangyong open-pit limestone mine in Korea, Energies (Basel). 9 (2016). https://doi.org/10.3390/en9020102.

[2] M.E. Taboada, L. Cáceres, T.A. Graber, H.R. Galleguillos, L.F. Cabeza, R. Rojas, Solar water heating system and photovoltaic floating cover to reduce evaporation: Experimental results and modeling, Renew Energy. 105 (2017) 601–615. https://doi.org/10.1016/j.renene.2016.12.094.

[3] R. Cazzaniga, M. Cicu, M. Rosa-Clot, P. Rosa-Clot, G.M. Tina, C. Ventura, Floating photovoltaic plants: Performance analysis and design solutions, Renewable and Sustainable Energy Reviews. 81 (2018) 1730–1741. https://doi.org/10.1016/j.rser.2017.05.269.

[4] J. Baptista, P. Vargas, J.R. Ferreira, A techno-economic analysis of floating photovoltaic systems, for southern european countries, Renewable Energy and Power Quality Journal. 19 (2021) 57–62. https://doi.org/10.24084/repqj19.214.

[5] R. Cazzaniga, M. Cicu, M. Rosa-Clot, P. Rosa-Clot, G.M. Tina, C. Ventura, Compressed air energy storage integrated with floating photovoltaic plant, J Energy Storage. 13 (2017) 48–57. https://doi.org/10.1016/j.est.2017.06.006.

[6] F. Piancó, L. Moraes, I. dos Prazeres, A.G.G. Lima, J.G. Bessa, L. Micheli, E. Fernández, F. Almonacid, Hydroelectric operation for hybridization with a floating photovoltaic plant: A case of study, Renew Energy. 201 (2022) 85–95. https://doi.org/10.1016/j.renene.2022.10.077.

[7] L. Liu, Q. Sun, H. Li, H. Yin, X. Ren, R. Wennersten, Evaluating the benefits of Integrating Floating Photovoltaic and Pumped Storage Power System, Energy Convers Manag. 194 (2019) 173–185. https://doi.org/10.1016/j.enconman.2019.04.071.

[8] K. Mongird, V. Viswanathan, J. Alam, C. Vartanian, V. Sprenkle, R. Baxter, 2020 Grid Energy Storage Technology Cost and Performance Assessment, Energy Storage Grand Challenge Cost and Performance Assessment 2020. (2020) 1–20. https://www.pnnl.gov/sites/default/files/media/file/PSH_Methodology_0.pdf.

[9] F. Bontempo Scavo, G.M. Tina, A. Gagliano, S. Nižetić, An assessment study of evaporation rate models on a water basin with floating photovoltaic plants, Int J Energy Res. 45 (2021) 167–188. https://doi.org/10.1002/er.5170.

[10] Jinko Solar, Tiger Pro 60HC 440-460 Watt Factsheet, (n.d.). https://www.jinkosolar.com/uploads/JKM440-460M-60HL4-(V)-F1-EN.pdf (accessed October 14, 2023).

[11] PVGIS Photovoltaic Geographical Information System, EU Science Hub - European Commission. (2018). https://ec.europa.eu/jrc/en/pvgis.

[12] W.C.L. Kamuyu, J.R. Lim, C.S. Won, H.K. Ahn, Prediction model of photovoltaic module temperature for power performance of floating PVs, Energies (Basel). 11 (2018). https://doi.org/10.3390/en11020447.

[13] B. Zakeri, S. Syri, Electrical energy storage systems: A comparative life cycle cost analysis, Renewable and Sustainable Energy Reviews. 42 (2015) 569–596. https://doi.org/10.1016/j.rser.2014.10.011.

[14] V. Ramasamy, R. Margolis, Floating Photovoltaic System Cost Benchmark: Q1 2021 Installations on Artificial Water Bodies, 2021. www.nrel.gov/publications.

[15] M. Catania, F. Parolin, F. Fattori, P. Colbertaldo, Impact of Detailed Hydropower Representation in National Energy System Modelling, (2023) 1947–1957. https://doi.org/10.52202/069564-0177.

[16] GME, GME - Esiti mercato elettrico, (n.d.). https://www.mercatoelettrico.org/it/Esiti/MGP/EsitiMGP.aspx.